

Structures of the Solvated Organic-Based Ferromagnet Decamethylferrocenium Tetracyanoethenide, $[\text{FeCp}^*_2]^+[\text{TCNE}]^- \cdot y\text{RCN}$ (R = Me, Et, *n*-Pr)

Joel S. Miller,^{*,†} Peter K. Gantzel,[‡] Arnold L. Rheingold,[‡] and Michelle L. Taliaferro[†]

Department of Chemistry, University of Utah, Salt Lake City, Utah 84112-0850, and Department of Chemistry, University of California, San Diego, La Jolla, California 92093-0358

Received January 14, 2009

The ferromagnet $[\text{FeCp}^*_2][\text{TCNE}]$ ($T_c = 4.80$ K) has two structural phase transitions at 249 and 282 K that has thwarted the determination of its structure by single crystal X-ray diffraction; however, its structure at 100 K is reported [$P2_1/c$, $a = 9.710(1)$ Å, $b = 14.214(2)$ Å, $c = 18.753(2)$ Å, $\beta = 113.207(2)^\circ$, $V = 2378.7(5)$ Å³, $Z = 4$, $T = 100$ K]. Because of the facile loss of solvent, the ferromagnetic solvates, $[\text{FeCp}^*_2][\text{TCNE}] \cdot y\text{S}$ {S = MeCN [$y = 1$, P , $a = 9.556(2)$ Å, $b = 9.781(2)$ Å, $c = 16.152(2)$ Å, $\alpha = 74.860(2)^\circ$, $\beta = 84.333(3)^\circ$, $\gamma = 65.030(4)^\circ$, $V = 1321.0(4)$ Å³, $Z = 2$, $T = 100$ K], EtCN [$y = 1/2$, $Pnma$, $a = 14.750(5)$ Å, $b = 10.577(5)$ Å, $c = 33.972(10)$ Å, $V = 5301(3)$ Å³, $Z = 8$, $T = 100$ K], *n*-PrCN [$y = 1/2$, $C2/m$, $a = 35.902(6)$ Å, $b = 10.488(2)$ Å, $c = 14.302(2)$ Å, $\beta = 101.396(3)^\circ$, $V = 5279(1)$ Å³, $Z = 8$, $T = 173$ K]} have also been difficult to crystallographically characterize, but have been determined from single crystal X-ray diffraction data. These structures consist of parallel chains of alternating $[\text{FeCp}^*_2]^+$ and $[\text{TCNE}]^-$ ions, with an intrachain Fe...Fe distance of 10.54 ± 0.09 Å. The solvates additionally possess chains of solvent that separate the alternating chains of $[\text{FeCp}^*_2]^+$ and $[\text{TCNE}]^-$ ions. The MeCN solvate forms layers of chains that separate two rows of chains, while the EtCN and *n*-PrCN solvates form chains surrounded by six chains, and have fewer nonmagnetic coupling pathways that result in higher ordering temperature with respect to the MeCN solvate.

Introduction

Decamethylferrocenium tetracyanoethenide, $[\text{FeCp}^*_2]^+[\text{TCNE}]^-$, **1**, was characterized to be a bulk three-dimensional (3-D) ferromagnet ($T_c = 4.80$ K) in the mid-1980s.^{1,2} The saturation magnetization of **1** is 37% more than that of iron metal on either an Fe or a mole basis, and its

discovery nucleated the study of organic-based magnets for which **1** is the prototype.³ Because of extensive structural disorder, the crystal structure of **1** could not be determined at room temperature, and upon cooling the crystals disintegrated,^{1c} as it underwent two structural phase transitions at 249 and 282 K.⁴ Recent, high-resolution powder diffraction studies using synchrotron radiation enabled the determination of (1) the temperature dependencies of the unit-cell parameters that are in accord with the reported phase transitions and (2) the Rietveld-refined structures of $[\text{FeCp}^*_2][\text{TCNE}]$ at 12, 250, and 295 K.⁵ As the temperature

* To whom correspondence should be addressed. E-mail: jsmiller@chem.utah.edu.

† University of Utah.

‡ University of California, San Diego.

- (1) (a) Miller, J. S.; Epstein, A. J.; Reiff, W. M. *Mol. Cryst. Liq. Cryst.* **1985**, *120*, 27. (b) Miller, J. S.; Calabrese, J. C.; Epstein, A. J.; Bigelow, R. W.; Zhang, J. H.; Reiff, W. M. *J. Chem. Soc., Chem. Commun.* **1986**, 1026. (c) Miller, J. S.; Calabrese, J. C.; Rommelmann, H.; Chittipeddi, S. R.; Zhang, J. H.; Reiff, W. M.; Epstein, A. J. *J. Am. Chem. Soc.* **1987**, *109*, 769. (d) Chittipeddi, S.; Cromack, K. R.; Miller, J. S.; Epstein, A. J. *Phys. Rev. Lett.* **1987**, *58*, 2695.
- (2) (a) Yee, G. T.; Miller, J. S. In *Magnetism - Molecules to Materials*; Miller, J. S., Drillon, M., Eds.; Wiley-VCH: Mannheim, 2004; Vol. 5, p 223. (b) Gama, V.; Duarte, M. T. In *Magnetism - Molecules to Materials*; Miller, J. S., Drillon, M., Eds.; Wiley-VCH: Mannheim, 2004; Vol. 5, p 1. (c) Coronado, E.; Galàn-Mascarós, J. R.; J. S. Miller, J. S. *Compr. Organomet. Chem.* **2006**, *12*, 413.

- (3) (a) Blundell, S. J.; Pratt, F. L. *J. Phys.: Condens. Matter* **2004**, *16*, R771. (b) Ovcharenko, V. I.; Sagdeev, R. *Z. Russ. Chem. Rev.* **1999**, *68*, 345. (c) Kinoshita, M. *Philos. Trans. R. Soc., A* **1999**, *357*, 2855. (d) Miller, J. S.; Epstein, A. J. *Chem. Commun.* **1998**, 1319. (e) Miller, J. S.; Epstein, A. J. *Chem. Eng. News* **1995**, *73#40*, 30. (f) Miller, J. S.; Epstein, A. J. *Angew. Chem., Int. Ed. Engl.* **1994**, *33*, 385. (g) Kinoshita, M. *Jpn. J. Appl. Phys.* **1994**, *33*, 5718. (h) Gatteschi, D. *Adv. Mater.* **1994**, *6*, 635.
- (4) Nakano, M.; Sorai, M. *Mol. Cryst. Liq. Cryst.* **1993**, *233*, 161.
- (5) Her, J.-H.; Stephens, P. W.; Ribas-Ariño, J.; Novoa, J. J.; Miller, J. S. *Inorg. Chem.* **2009**, *49*, 0000; DOI: 10.1021/ic801679m.

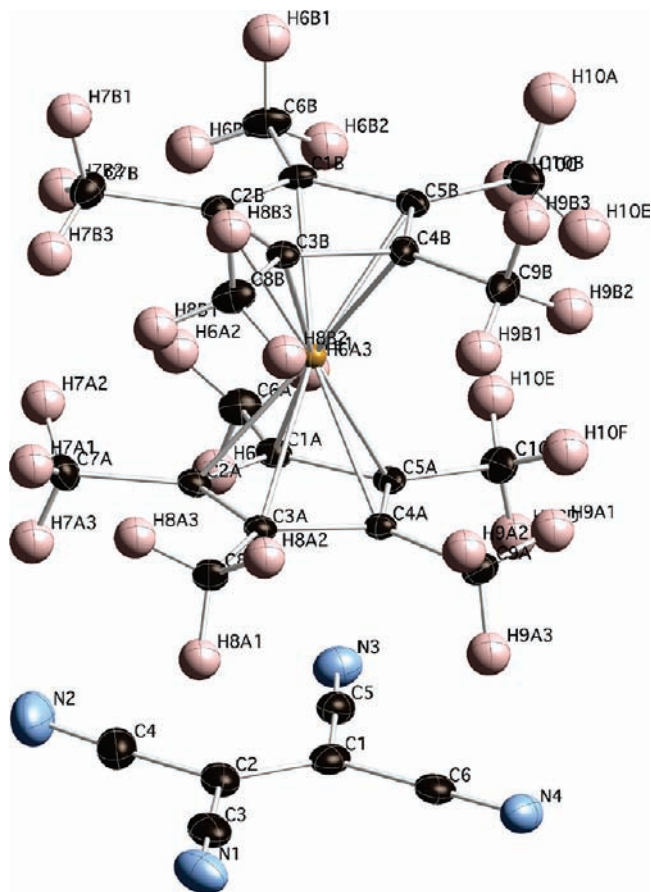


Figure 1. ORTEP (30%) atom labeling diagram of $[\text{FeCp}^*_2][\text{TCNE}]$ at 100 K.

is decreased the structures became less disordered, but the overall motif of parallel chains of alternating radical $[\text{FeCp}^*_2]^+$ cations (C^+) and radical $[\text{TCNE}]^-$ anions (A^-), which are in- and out-of-registry with respect to each other, is maintained. This is the structure of **1** and of desolvated **1**·MeCN for which its magnetic properties have been extensively studied for the past two decades.

The structure of $[\text{FeCp}^*_2]^+[\text{TCNE}]^- \cdot \text{MeCN}$ (**1**·MeCN) was determined at 243 K, and possesses two rows of parallel chains of alternating C^+ and A^- ions separated by a layer of chains of MeCN solvent.^{1c} Because of the facile loss of the MeCN from this solvate, its magnetic properties are that of desolvated **1**, unless special precautions are taken. The magnetic behavior of **1**·MeCN was only recently determined via using excess solvent in equilibrium with the crystals.⁶ **1**·MeCN also orders as a ferromagnet, but with a significantly increased magnetic glassiness, and a magnetic ordering temperature reduced by 42% to 2.87 K. These differences are attributed to the reduced nearest-neighbor coupling arising from layers of MeCN that separate some of the chains of alternating radical ions. Likewise other solvates (EtCN, *n*-PrCN, PhCN, 1,2- $\text{C}_6\text{H}_4\text{Cl}_2$, and $\text{NCC}_4\text{H}_8\text{CN}$) also exhibit reduced ordering temperatures.⁶ Herein, we report the stoichiometry, as well as structures, of the EtCN and *n*-PrCN solvates of **1**, the determination of the structure of a different

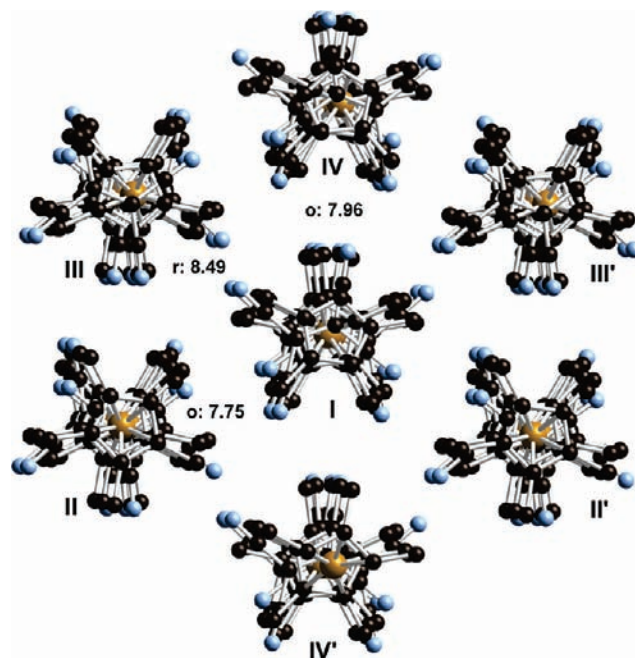


Figure 2. Top-view showing the unique adjacent parallel chains of $[\text{FeCp}^*_2][\text{TCNE}]$ (**1**) at 100 K and their interchain separations (*r*: in-registry chains; *o*: out-of-registry chains).

phase of the **1**·MeCN solvate at 100 K, and the unexpected determination of the structure of solvent-free **1** at 100 K.

Experimental Section

1·S (*S* = MeCN, EtCN, *n*-PrCN) was prepared as previously reported, and crystals in the mother liquor formed upon cooling a saturated solution to -30°C .⁶ The cold crystals with mother liquor were poured onto a paper towel, and crystals were quickly plucked with Paratone oil on a needle, then placed onto a Paratone drop on a microscope slide, and subsequently mounted for study. While not all crystals were suitable for diffraction studies, this process was repeated until suitable crystals were identified.

In this manner the single-crystal X-ray structure determinations of **1** and **1**·S (*S* = MeCN, EtCN, *n*-PrCN) were solved by standard techniques using either direct methods or the Patterson heavy-atom method, which yielded the position of the Fe atom. The remaining atoms were located in subsequent Fourier difference maps. A summary of the experimental conditions is presented in Table 1. Non-hydrogen atoms were refined anisotropically, and hydrogen atoms were treated as idealized contributions. All software used is contained in the APEX, SAINT, and SHELXL libraries maintained by Bruker-AXS (Madison, WI).

Results and Discussion

The reaction of $\text{Fe}^{\text{II}}\text{Cp}^*_2$ and TCNE forms the electron transfer salt $[\text{Fe}^{\text{III}}\text{Cp}^*_2]^+[\text{TCNE}]^-$, **1**, which depending on the solvent (*S*) can form a crystalline solvate, $[\text{FeCp}^*_2][\text{TCNE}] \cdot y\text{S}$, **1**·S.^{1c} The solvent is very easily lost upon standing at room temperature and forms **1**, with a concomitant structural change, as confirmed from X-ray^{1c} and magnetic studies.⁶ **1**·S is only stable in equilibrium in the presence of excess *S*, and studying the crystals in this equilibrium enabled their frequency-dependent alternating current (AC) magnetic properties, including the magnetic freezing temperature, T_f , to be determined.⁶ Using the

(6) Taliaferro, M. L.; Selby, T. D.; Miller, J. S. *Chem. Mater.* **2003**, *15*, 3602.

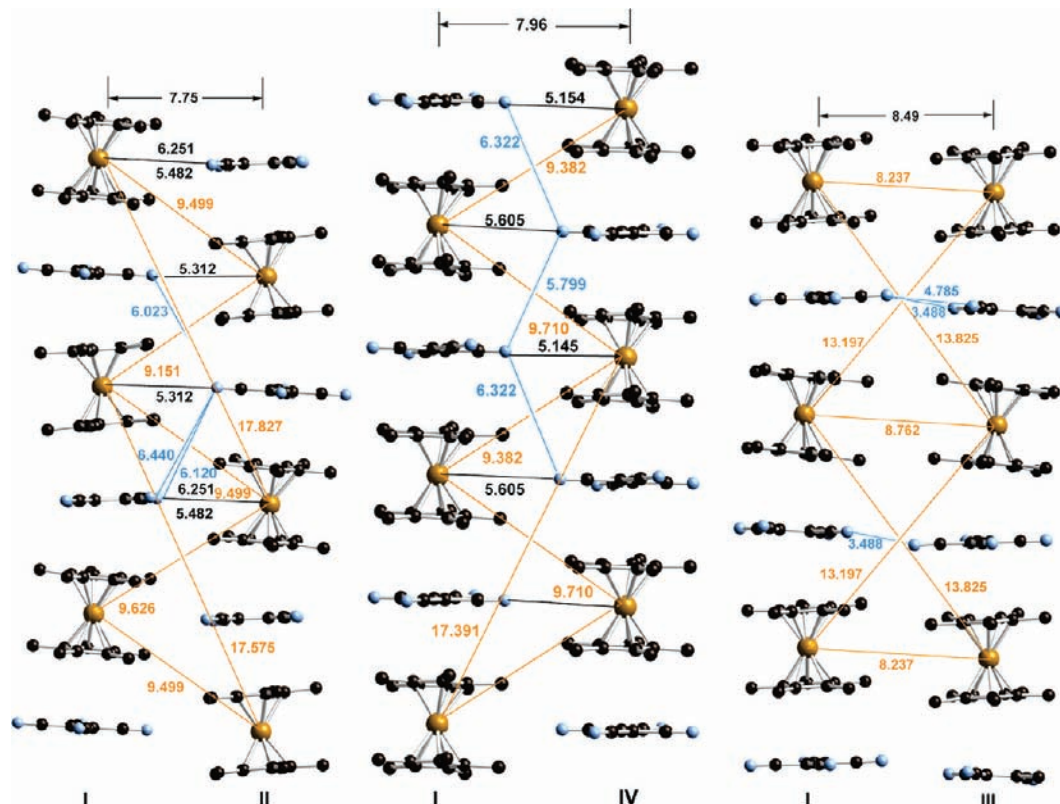


Figure 3. Adjacent out-of-registry (o) I–II, I–IV, and in-registry (r) I–III parallel chains of **1** at 100 K and their interchain separations.

Table 1. Summary of the Crystallographic Parameters for $[\text{FeCp}^*_2][\text{TCNE}]$ and $[\text{FeCp}^*_2][\text{TCNE}] \cdot \text{S}$ (S = MeCN, EtCN, *n*-PrCN).

<i>y</i> S	none	MeCN	1/2(EtCN)	1/2(<i>n</i> -PrCN)
empirical formula	$\text{C}_{26}\text{H}_{30}\text{FeN}_4$	$\text{C}_{28}\text{H}_{33}\text{FeN}_5$	$\text{C}_{27.5}\text{H}_{32.5}\text{FeN}_{4.5}$	$\text{C}_{28}\text{H}_{33.5}\text{FeN}_{4.5}$
MW, dalton	454.39	495.44	481.93	488.94
<i>T</i> (K)	100(2)	100(2)	100(2)	173(2)
<i>a</i> (Å)	9.7095(12)	9.556(2)	14.752(5)	35.902(6)
<i>b</i> (Å)	14.2142(18)	9.781(2)	10.577(5)	10.4884(16)
<i>c</i> (Å)	18.753(2)	16.152(2)	33.972(10)	14.302(2)
α (deg)	90	74.860(3)	90	90
β (deg)	113.207(2)	84.333(3)	90	101.396(3)
γ (deg)	90	65.030(4)	90	90
<i>V</i> (Å ³)	2378.7(5)	1321.0(4)	5301(3)	5279.0(14)
<i>Z</i>	4	2	8	8
space group	$P2_1/c$	$P\bar{1}$	$Pnma$	$C2/m$
ρ , calc(g cm ⁻³)	1.268	1.246	1.208	1.230
R1 [<i>I</i> > 2 $\sigma(I)$] ^a	0.0438	0.0594	0.0796	0.1141
wR2 [<i>I</i> > 2 $\sigma(I)$] ^b	0.1059	0.1618	0.1969	0.2131
goodness of fit (<i>F</i> ²)	0.993	1.160	0.995	1.254
largest diff. peak/hole, e Å ⁻³	0.927/−0.492	0.768/−0.831	0.605/−0.791	0.762/−1.079

technique of rapidly pouring the crystals and its saturated solution onto a piece of paper, and then promptly coating the crystallites with Paratone oil to minimize both solvent loss and exposure to air, led to the crystals of **1**·S that were of sufficient quality to enable their structures to be determined. In one fortunate, but unexpected, case crystalline solvent-free **1** was studied. The protected crystals were mounted and their structures determined at low temperature.

Because of the facile loss of S, the stoichiometry of **1**·S could only be ascertained from the structural determination. The structurally determined stoichiometries for $[\text{FeCp}^*_2][\text{TCNE}] \cdot y\text{S}$ are as follows: S = MeCN, *y* = 1; S = EtCN, *y* = 1/2; and S = *n*-PrCN, *y* = 1/2.

$[\text{FeCp}^*_2][\text{TCNE}]$. The structure of **1** crystallizes in the monoclinic $P2_1/c$ space group as reported for its structure

determined at 12 K from the Rietveld refinement of the powder X-ray diffraction data,⁵ and its atom labeling diagram is presented in Figure 1. Above ~249 K **1** possesses the $P2_1/m$ space group.⁵ The structure consists of parallel chains of alternating C^{*+} and A^{*-} ions with an intrachain $\text{Fe} \cdots \text{Fe}$ separation of 10.514(2) Å. This motif has four unique pairs of chains (Figure 2): out-of-registry I–II, I–IV, and in registry I–III, and their key interatomic separations are noted in Figure 3. These values are comparable to that observed at 12 K, and, overall, the intra- and interchain $\text{Fe} \cdots \text{Fe}$ separations decrease on cooling to 12 K by $0.5 \pm 0.1\%$ (0.6%/100 K). In addition to the expected contraction, the chains become more tilted upon cooling. The tilting arises from the mean plane of the $[\text{TCNE}]^-$ tilting away from the Cp* mean plane, Figure 4, such that half of the eight $\text{Fe} \cdots \text{N}$

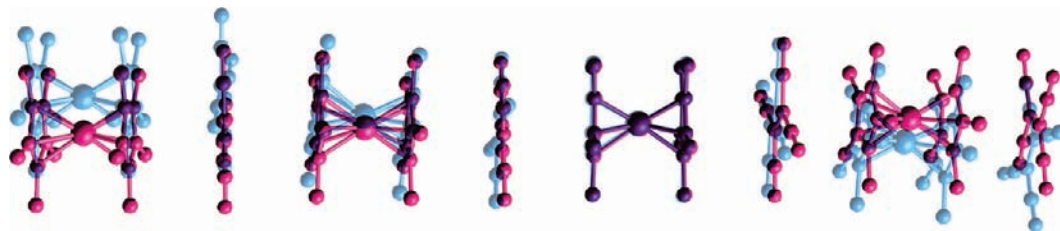


Figure 4. $[\text{FeCp}^*_2][\text{TCNE}]$ chain segment at 12 K (blue) overlaid with its arrangement at 100 K (red) showing the tilting.

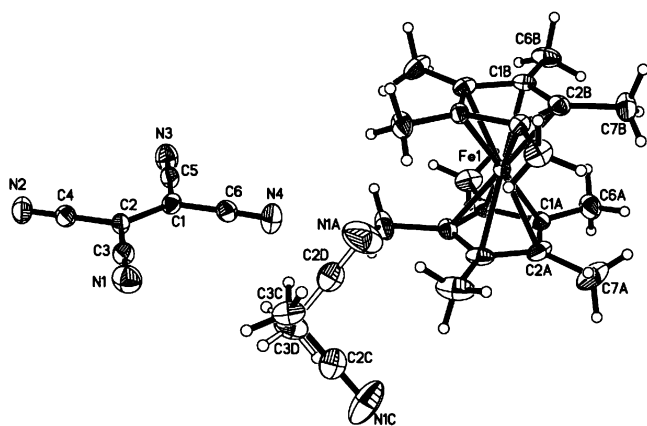


Figure 5. ORTEP (30%) atom labeling diagram of $[\text{FeCp}^*_2][\text{TCNE}] \cdot \text{MeCN}$ ($1 \cdot \text{MeCN}$).

separations increase (average = 0.8%) and half-decrease on cooling (by 2.2%), with the average $\text{Fe} \cdots \text{N}$ separations decreasing by an average of 0.7%.

$[\text{FeCp}^*_2][\text{TCNE}] \cdot \text{MeCN}$, $1 \cdot \text{MeCN}$. The structure of $1 \cdot \text{MeCN}$ was determined at 100 K and qualitatively differs from that determined at 243 K,^{1c} and its atom labeling diagram is shown in Figure 5. While both the cation and anion are structurally ordered, the solvent is disordered over two orientations in nearly a 50:50 ratio. Both solvent molecule orientations are located near the inversion centers. At 243 K the space group is $C2/c$ with eight molecules per unit cell, whereas at 100 K it becomes $P\bar{1}$ with two molecules per unit cell. At both temperatures the alternating C^{*+} and A^{*-} chain arrangement remains the same, but the intrachain $\text{Fe} \cdots \text{Fe}$ separation decreases very slightly from 10.415(3) to 10.396(4) Å. The overall arrangement of the parallel chains and location layers of the MeCN solvent are similar in each phase, and there are two rows of $[\text{FeCp}^*_2][\text{TCNE}]$ chains followed by a layer of solvent, Figure 6. Although cooling leads to a phase change, the structural motif remains nominally the same except for the expected contractions because of cooling.

$[\text{FeCp}^*_2][\text{TCNE}] \cdot 1/2(\text{EtCN})$. The structure of $1 \cdot 1/2(\text{EtCN})$ crystallizes at 100 K in the orthorhombic space group $Pnma$, and an analysis of the stoichiometry reveals an Fe/EtCN ratio of 2:1; hence, it differs from $1 \cdot \text{MeCN}$. The atom labeling diagram is shown in Figure 7 and shows the two unique Fe sites as well as $[\text{TCNE}]^{*-}$, one ordered and one disordered over two orientations. Likewise, the solvent and one of the independent $[\text{TCNE}]^{*-}$ are disordered about the crystallographic mirror plane. As occurs for **1** and $1 \cdot \text{MeCN}$, $1 \cdot 1/2(\text{EtCN})$ possesses parallel chains of alternating C^{*+} and A^{*-} ions, with a comparable intrachain $\text{Fe} \cdots \text{Fe}$ separation of 10.577(3) Å. In contrast to $1 \cdot \text{MeCN}$, the

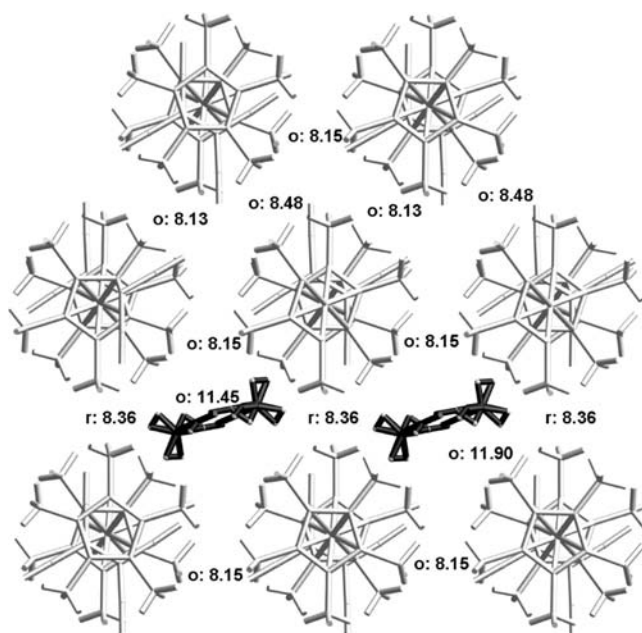


Figure 6. Packing of adjacent chains of alternating $[\text{FeCp}^*_2]^+$ and $[\text{TCNE}]^-$ in $1 \cdot \text{MeCN}$ at 100 K and their interchain separations (r: in-registry chains; o: out-of-registry chains). Every second layer of rows of $[\text{FeCp}^*_2][\text{TCNE}]$ is separated by layers of the MeCN solvent.

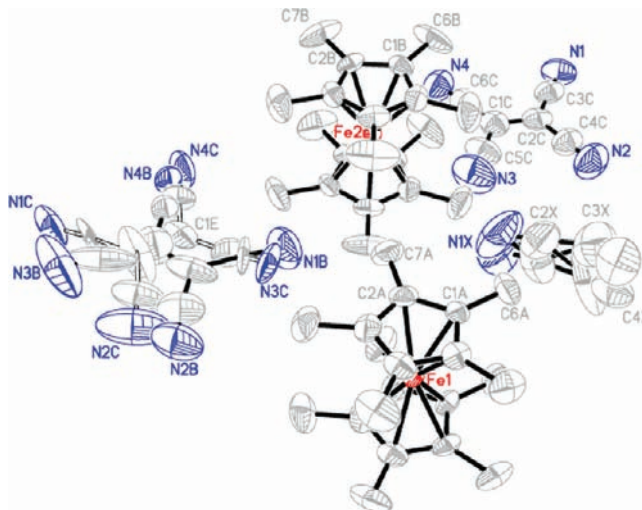


Figure 7. ORTEP (30%) atom labeling diagram of $[\text{FeCp}^*_2][\text{TCNE}] \cdot 1/2(\text{EtCN})$.

solvent in $1 \cdot 1/2(\text{EtCN})$ resides in channels that are surrounded by six chains of alternating $[\text{FeCp}^*_2]^+$ and $[\text{TCNE}]^-$ ions, Figure 8.

The nearest neighbor chains separations that range from 7.67 to 8.92 Å are comparable to that observed for **1** (7.75 to 8.49 Å). The separations, however, increase when separated by the solvent to 9.14 and 11.20 Å

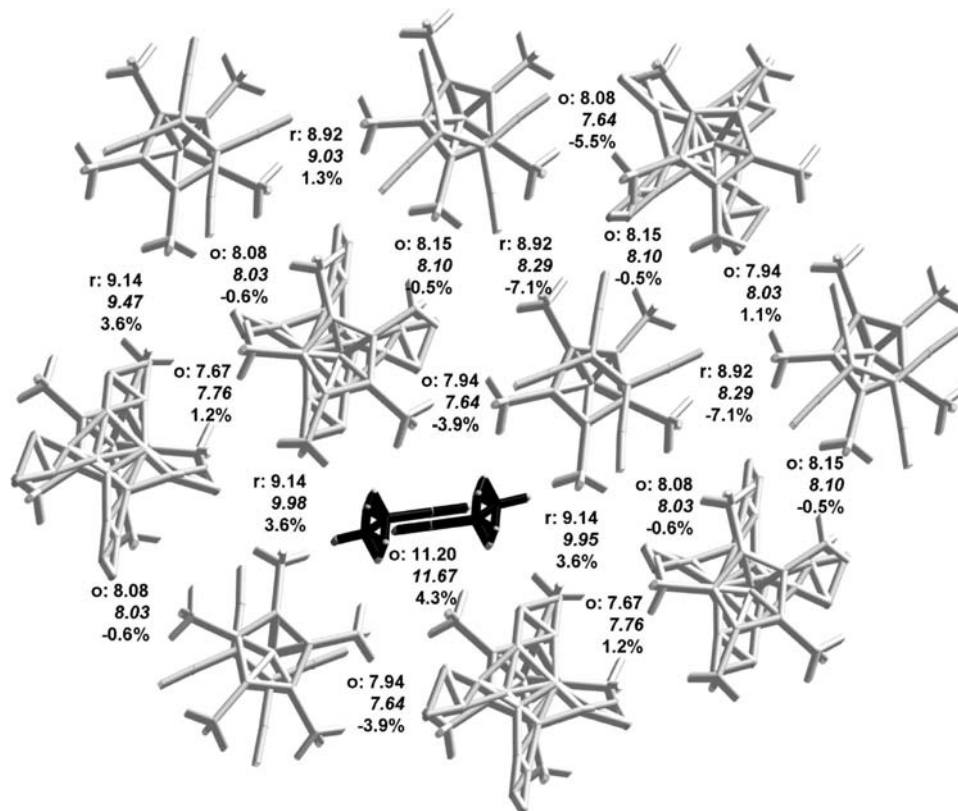


Figure 8. Packing of adjacent chains of alternating $[\text{FeCp}^*_2]^{2+}$ and $[\text{TCNE}]^{1-}$ in $1 \cdot 1/2\text{S}$ ($\text{S} = \text{EtCN}, n\text{-PrCN}$) at 100 K. The top values are the interchain separations (r: in-registry chains; o: out-of-registry chains) for $\text{S} = \text{EtCN}$, while the italicized values are for $\text{S} = n\text{-PrCN}$, and percent change is noted below. The solvent (EtCN or $n\text{-PrCN}$) resides in channels that are surrounded by six chains of alternating $[\text{FeCp}^*_2]^{2+}$ and $[\text{TCNE}]^{1-}$ ions.

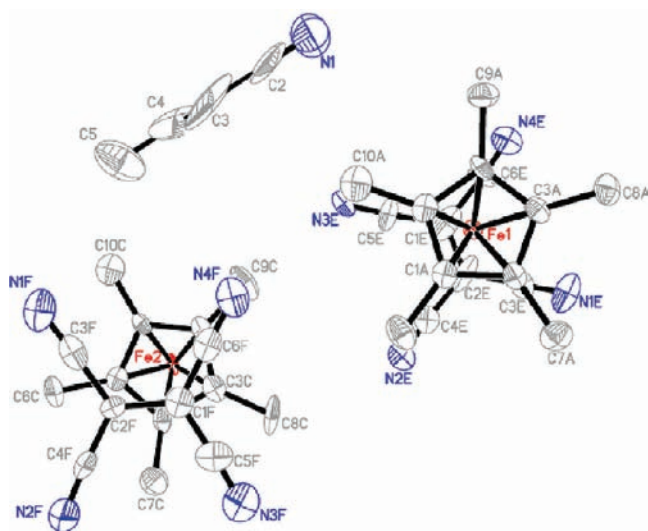


Figure 9. ORTEP (30%) atom labeling diagram of $[\text{FeCp}^*_2][\text{TCNE}] \cdot 1/2(n\text{-PrCN})$.

$[\text{FeCp}^*_2][\text{TCNE}] \cdot 1/2(n\text{-PrCN})$. The structure of $1 \cdot 1/2(n\text{-PrCN})$ crystallizes at 173 K in the monoclinic space group $C2/m$, and an analysis of the stoichiometry reveals an $\text{Fe}/n\text{-PrCN}$ ratio of 2:1; hence, it is similar to $1 \cdot 1/2(\text{EtCN})$ and differs from $1 \cdot \text{MeCN}$. The atom labeling diagram is shown in Figure 9 and shows the two unique Fe sites as well as $[\text{TCNE}]^{1-}$. The solvent is disordered equally about the crystallographic mirror plane. As occurs for **1**, $1 \cdot \text{MeCN}$, and $1 \cdot 1/2(\text{EtCN})$, $1 \cdot 1/2(n\text{-PrCN})$ also possesses parallel chains of alternating C^{2+} and A^{1-} ions, with a comparable

intrachain $\text{Fe} \cdots \text{Fe}$ separation of $10.488(2) \text{ \AA}$. In contrast to $1 \cdot \text{MeCN}$ but similar to $1 \cdot 1/2(\text{EtCN})$ the $n\text{-PrCN}$ resides in channels that are surrounded by six chains of alternating $[\text{FeCp}^*_2]^{2+}$ and $[\text{TCNE}]^{1-}$ ions, Figure 8. The nearest neighbor chains are separated by 7.76 to 9.03 \AA . The separations, however, increase when separated by the solvent to 9.47 and 11.67 \AA . These values are very comparable to that observed for $1 \cdot 1/2(\text{EtCN})$.

Although $1 \cdot 1/2(\text{EtCN})$ and $1 \cdot 1/2(n\text{-PrCN})$ belong to two different space groups, they have an almost identical 3-D structural motif, Figure 8. The intrachain interactions are comparable for $1 \cdot 1/2(\text{EtCN})$ and $1 \cdot 1/2(n\text{-PrCN})$ as well as **1** and $1 \cdot \text{MeCN}$. Both $1 \cdot 1/2(\text{EtCN})$ and $1 \cdot 1/2(n\text{-PrCN})$ have columns of solvent (disordered) that are surrounded by six chains of alternating C^{2+} and A^{1-} ions. The nearest neighbor interchain separations are shown in Figure 8 for $1 \cdot 1/2(\text{EtCN})$ and $1 \cdot 1/2(n\text{-PrCN})$ and differ in their separations from -7.1 to 4.3% (average change is 0.6%).

Magnetic ordering is attributed to the chain motif that yields intra- and interchain ferromagnetic coupling.^{1,5} The presence of layers of MeCN or isolated chains of EtCN or $n\text{-PrCN}$ solvent increase the interchain separation reducing the interchain couplings that are essential for 3-D magnetic ordering. The greatest reduction in ordering temperature occurs for MeCN , which forms layers of chains that separate two rows of chains, while the EtCN and $n\text{-PrCN}$ solvates form chains surrounded by six chains, and have fewer nonmagnetic coupling pathways that result in a higher ordering temperature with respect to the MeCN solvate, as

is observed.⁶ These, however, are ordering temperatures that are reduced with respect to the nonsolvated material, **1**. The detailed structural parameters enable computational studies to identify magnetostructural trends that are in progress.

Conclusion

While $[\text{FeCp}^*_2]^{2+}[\text{TCNE}]^{-}$ and $[\text{FeCp}^*_2]^{2+}[\text{TCNE}]^{-} \cdot \text{MeCN}$ were synthesized more than two decades ago, their crystal structures have been challenging to obtain. Cooling crystals to obtain low temperature crystallographic data failed for single crystals because of disintegration of the crystals but permitted their study by powder diffraction.⁵ Nonetheless, a crystal of **1** was grown at low temperature and structurally determined by a single crystal study at 100 K. The solvates, which also magnetically order,⁶ undergo facile loss of solvent, but methodology to capture these crystals was identified, and the MeCN, EtCN, and *n*-PrCN solvents were structurally characterized. All

of its structures or those of its solvates possess parallel chains of alternating $[\text{FeCp}^*_2]^{2+}$ and $[\text{TCNE}]^{-}$ ions, with an intrachain Fe...Fe distance of $10.54 \pm 0.09 \text{ \AA}$.^{1c,5}

Acknowledgment. We are grateful for useful discussions with Peter W. Stephens and Jae-Hyuk Her (Stony Brook University). We acknowledge the continued partial support from the U.S. DOE (No. DE FG 03-93ER45504) and the AFOSR (No. F49620-03-1-0175).

Supporting Information Available: Crystallographic data (atomic positions, thermal parameters, bond lengths, the raw powder diffraction data and fitted profiles) for **1**, **1**·MeCN, **1**·1/2(EtCN), and **1**·1/2(*n*-PrCN) in the form of CIF files (CCDC#716105–716108). This material is available free of charge via the Internet at <http://pubs.acs.org>.

IC900075J